

The SiPM revolution in time-domain diffuse optics

Alberto Dalla Mora^{a*}, Laura Di Sieno^a, Anurag Behera^a, Paola Taroni^{a,b}, Davide Contini^a,
Alessandro Torricelli^{a,b}, Antonio Pifferi^{a,b}

^aPolitecnico di Milano, Dipartimento di Fisica, Piazza Leonardo da Vinci 32, 20133, Milano, Italy

^bConsiglio Nazionale delle Ricerche, Istituto di Fotonica e Nanotecnologie, Piazza Leonardo da Vinci 32, 20133
Milano, Italy

*Corresponding author: alberto.dallamora@polimi.it, Politecnico di Milano, Dipartimento di Fisica, Piazza
Leonardo da Vinci 32, 20133, Milano, Italy, Phone: +39 02 2399 6108, Fax: +39 02 2399 6126

Abstract: Time-domain diffuse optics is a powerful non-invasive, non-ionizing and label-free technique based on the use of picosecond pulsed laser light to probe highly scattering media like biological tissues down to a depth of few centimeters to obtain functional and compositional information. This technique is opening new perspectives in various fields spanning from oncology (e.g. characterization of breast or thyroid lesions, etc.) to neurology (e.g. diagnosis and monitoring of traumatic brain injuries, functional brain imaging, etc.), as well as in non-biomedical fields (e.g. characterization of fruits, wood, etc.). Time-domain diffuse optics is nowadays undergoing fascinating technology advancements, permitting for the first time the design of low-cost compact/wearable high performance systems. This revolution has been made possible also taking advantage from Silicon PhotoMultiplier (SiPM) progresses, originally driven by other applications, since time-domain diffuse optics is highly demanding in terms of performance, in particular requiring single-photon detectors with large collection area, high fill-factor, high single-photon timing resolution, low power dissipation and compact high-throughput front-end electronics. This work will review the recent advancements introduced by SiPMs in time-domain diffuse optics, mostly thanks to the support of different running EU H2020 projects (e.g. SOLUS -G.A.731877-, LUCA -G.A.688303-, BITMAP -G.A.675332-, ATTRACT -G.A.777222-, Laserlab-Europe -G.A.654148-), showing their present performances in this field, the inherent advantages that allowed the design of innovative diffuse optical imaging systems, as well as highlighting their present limitations in order to push forward the research towards the perfect SiPM for time-domain diffuse optics.

Keywords: time-domain diffuse optics, silicon photomultiplier, single-photon avalanche diode, photon scattering, near-infrared spectroscopy, time-correlated single-photon counting.

1 Introduction

The use of light for probing highly scattering media (i.e. diffuse optics, -DO-) is drawing attention in different biomedical and not biomedical fields [1]-[5]. Many different biological media are quite transparent in the wavelength range between 600 and 1100 nm as scattering dominates with respect to absorption, leading to the possibility to probe them down to a depth of 2-3 cm when a reflectance geometry measurement scheme is adopted [6]. In this scheme, light is injected and collected at the same side of the medium under investigation, with certain distance between such points (ρ). By exploiting light sources at different wavelengths it is possible to retrieve the absorption (μ_a) and reduced scattering coefficients (μ'_s) spectra of the medium, respectively linked to its chemical composition and microstructure [7]. This opens up to a plenty of applications like: functional brain imaging or muscle oximetry (where the technique commonly takes the name of functional Near-Infrared Spectroscopy -fNIRS-) [8], optical mammography [9], thyroid nodules characterization [10], bone pathologies examinations [11] as

47 well as non-biomedical applications like the non-destructive quality assessment of food [12],
48 wood [13], pharmaceutical [14] and semiconductor powders [15]. As DO only relies on the use
49 of light, the technique is non-invasive, non-ionizing and label-free. Depending on the different
50 possible light modulation, one can operate a DO system in different ways. Among the most
51 common adoptions it is worth mentioning the continuous-wave (CW) regime, the time-domain
52 (TD) and the frequency-domain (FD) [16]. It is well known that CW DO is the simplest
53 approach to the measurement, but at the same time the information content of a measurement
54 performed with a single source-detector pair is the lowest. On the other side, among other
55 techniques TD DO is the most demanding in terms of cost and complexity of the
56 instrumentation, but the information content of a single measurement is the highest [16]. In
57 particular, by monitoring just the intensity of light backscattered by the tissue, a single CW DO
58 channel cannot disentangle μ_a and μ'_s information. Instead, TD DO relies on the injection of light
59 pulses in the picosecond range and time-resolved detection of single-photons re-emitted by the
60 medium under investigations, followed by their classification with Time-Correlated Single-
61 Photon Counting technique (TCSPC) [17]. The re-emitted light pulse at a certain source-detector
62 separation from the injection point is broadened and attenuated due to both scattering and
63 absorption. However, as scattering mainly affects the pulse width and delay, while absorption
64 mainly affects the pulse decay tail, μ_a and μ'_s can be separately assessed [16]. For this reason,
65 TD DO is also less prone to motion artifacts as they often result into a signal attenuation, which
66 can be detrimental only for CW DO. Additionally, using CW DO the penetration depth is
67 dependent on the source-detector distance ρ . Hence, depth penetration can be increased by
68 increasing ρ , at the expenses of the signal-to-noise ratio, as the signal level exponentially
69 decreases upon increasing ρ , thus resulting into a trade-off between signal level and depth
70 penetration. On the contrary, with TD DO the average investigated depth is: i) independent of ρ
71 (thus allowing the use of short ρ to increase the signal instead of forcing the use of large ρ as in
72 the case of CW DO) [18] and ii) encoded in the photons' time of flight [19],[20]. It is therefore
73 sufficient to analyze photons detected at longer delays with respect to the injection time of the
74 laser pulse into the medium to maximize the penetration depth. For this reason, TD DO shows
75 the highest depth selectivity when there is the need to disentangle information about structures
76 set at different depths inside biological tissues (e.g. in disentangling hemodynamic changes
77 occurring within skin/skull and those occurring in the brain) [21]. It has been first theorized [22]
78 and then demonstrated [23],[24] that one can even adopt a null or small (few mm) ρ , adding
79 further advantages to the TD approach. First, the volume probed in the medium (i.e. the
80 sensitivity shape) is much more symmetrical and confined, acquiring a drop-like shape instead of
81 the classical banana-like shape [23], thus increasing the spatial resolution of the technique.
82 Moreover, as more photons result confined into a smaller volume, the contrast produced by a
83 possible localized perturbation (e.g. a localized functional activation of the brain, as well as a
84 tumor) inside the sensitivity shape and the number of photons reaching the detector are higher at
85 all the arrival delays with respect to the laser injection time within the tissue [23]. Unfortunately,
86 upon decreasing ρ , the amount of early-arriving photons increases much faster than that of late
87 photons, thus increasing the information related to the outer regions of the probed volume, up to
88 the saturation of the single-photon detection chain. Pushing this up to the limit (i.e. null ρ , where
89 the source and detector are in the same point, as it can be achieved with a single fiber [25]) the
90 direct reflection from medium surface is detected. Being a few percent fraction of the injected
91 light, this signal results extremely above the single-photon regime. In these condition, a time-
92 gated photon-detection scheme should be adopted, using single-photon detectors that can survive

93 to trillions of photons impinging during the OFF state (i.e. early-photons), with quite unaltered
94 performance in the following ON state, where late-photons must be recorded. Up to now, this has
95 been possible only using single-photon avalanche diodes (SPADs) [26],[27] (i.e. the main
96 building block of the silicon photomultiplier, SiPM) as the photocathode of intensified
97 photomultiplier tubes (PMTs) can be damaged by high photon fluxes. In the following, we take
98 advantage of the expertise and collaborations of our research group to provide an overview of the
99 recent technological advancements in TD DO, focusing in particular on those introduced by
100 SiPMs, mostly thanks to the support of different running EU H2020 projects (e.g. SOLUS [28],
101 LUCA [29], BITMAP [30], ATTRACT [31], Laserlab-Europe [32]), showing their present
102 performances in this field, the inherent advantages that allowed the design of innovative diffuse
103 optical imaging systems, as well as highlighting their present limitations in order to push forward
104 the research towards the perfect SiPM for TD DO.
105

106 **2 State of the art and trends**

107 Table 1 shows the main theoretical and practical advantages and disadvantages of TD DO before
108 2015, which represents the starting point of a revolution in the field, with fast technological
109 advancements that are still running. The expected features of next generation of TD DO devices
110 is shown after 2020 for comparison. As discussed above, with respect to CW DO, TD DO allows
111 to freely set the ρ as the investigated depth does not depend on this choice. Thus, theoretically,
112 many measurement points can be arranged into a small area allowing to fabricate dense
113 measurements grids, with no gap between sources and detectors. Additionally, as a small p
114 approach allows to confine the sensitivity shape within the medium as well as to increase the
115 number of photons collected at all the arrival delays, the operation in the TD allows higher
116 spatial resolution and sensitivity to deeper structures. Thanks to the possibility to analyze
117 photons arriving with different delays to retrieve information coming from different depths, TD
118 DO has the highest depth selectivity. Finally, exploiting an information encoded in the shape of
119 the re-emitted pulse, TD DO results more informative with respect to CW DO, and less prone to
120 motion artifacts.

121 As a matter of fact, despite decades of research in TD DO, only CW and FD devices have
122 pervaded the market of biomedical optics. It is worth noting that, to the best of our knowledge,
123 there is only one company on the market (in Japan) with TD fNIRS devices [33]. The main
124 reasons behind this are listed in the bottom rows of Table 1. TD instrumentation is much more
125 expensive and bulky with respect to CW devices. Hence, the adoption of a large number of
126 collection points similar to cutting-edge CW systems recently reported in the literature [34] are
127 not feasible at the moment in a TD approach. For the above mentioned reasons, before 2015
128 devising wearable and/or battery-operated TD systems was considered science fiction.

129 As a matter of fact, TD DO instruments underwent strong technological advances already well
130 before 2015. Two decades ago, for instance, first TD instruments were indeed based on bulky,
131 delicate and expensive titanium sapphire lasers [35]. Then, new sources appeared on the market
132 like supercontinuum pulsed fiber lasers or pulsed diode lasers. Exploiting these technologies, it
133 was possible to fabricate rack-based TD systems, for the first time suitable to enter in the clinical
134 environment [8], as well as to fabricate first TD multichannel systems for topographic or
135 tomographic optical imaging [36]-[39]. Still, the high fabrication cost (in the order of hundred

136 thousand euros) as well as the fridge-like dimension, prevented a widespread adoption of these
 137 technologies in both the research environment and, consequently, in the clinical practice.

138
 139

140 **Table 1** Advantages of TD DO before the SiPM revolution and its future perspective after 2020.

141

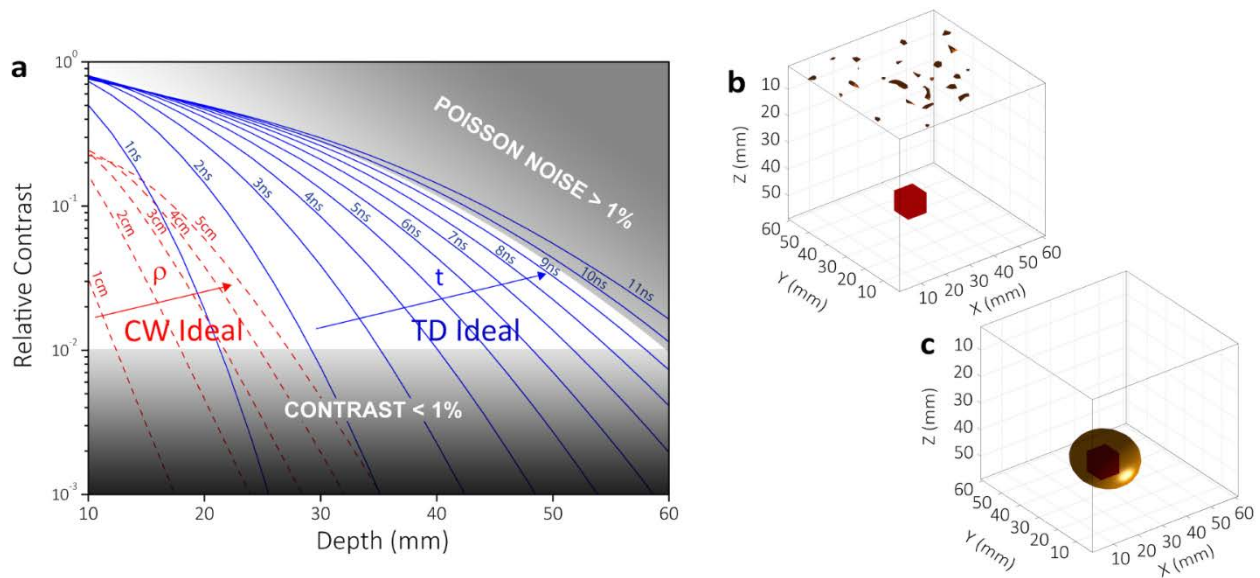
FEATURE	Time Domain (before 2015)	Time Domain (after 2020)
Free selection of ρ	YES	YES
Dense grid of measurement points	YES	YES
High spatial resolution	YES	YES
High depth sensitivity	YES	YES
High depth selectivity	YES	YES
High accuracy	YES	YES
Low Cost	NO	YES
Compact	NO	YES
Many parallel channels	NO	YES
Wearable	NO	YES
Battery operated	NO	YES

142
 143

144 It is worth nothing that the miniaturization of TD systems down to wearable devices is attractive
 145 not only due to an increased versatility, but also for increasing the performances. Indeed,
 146 although photocathode-based detectors can exhibit active areas of different square millimeters,
 147 practically they cannot be used in contact with the tissue under investigation, thus requiring the
 148 use of optical fibers to drive the light from the collection point on the sample to the detector,
 149 limiting both the collection area and the numerical aperture, often losing more than one order of
 150 magnitude of useful signal.

151 Figure 1 shows a simulated comparison between the ultimate performance achievable by CW
 152 and TD techniques [40]. For this purpose, the simulated ideal scenario doesn't take into account
 153 any technological limitation assuming for instance for TD the possibility to use a detector with
 154 delta-Dirac timing response, 100% photon detection efficiency and a large active area of 1 cm²,
 155 in direct contact with the tissue under investigation to avoid signal losses, with perfect time-
 156 gating capability to reject early-arriving photons. Equivalently, on the source side, it is assumed
 157 the possibility to use the maximum amount of laser light that can be injected in the tissue in an
 158 area of 1 cm² without overcoming the maximum permissible exposure limits for skin. A high
 159 throughput timing electronics is considered, so as to avoid any loss due to the saturation of the

160 digital stage that allows to retrieve the distribution of the photons' time of flight. For CW,
 161 different ρ (expressed in cm in Figure 1) are considered, so as to enable probing tissues at
 162 different depths. For TD, only null ρ is simulated, as the depth selectivity is ensured thanks to the
 163 possibility to process photons at the different arriving delays (in ns in Figure 1). In Figure 1a it is
 164 simulated the contrast (i.e. the relative change in the number of photon counts [40]) produced by
 165 a localized absorption perturbation ($\Delta\mu_a = 0.1 \text{ cm}^{-1}$) set at different depths inside a homogeneous
 166 scattering medium characterized by $\mu_a = 0.1 \text{ cm}^{-1}$ and $\mu'_s = 10 \text{ cm}^{-1}$. The shadowed regions limit
 167 the detectability where contrast is $> 1\%$ (which is considered distinguishable within the
 168 biological variability) and where the Poisson noise does not exceed 1%, so that the contrast is
 169 statistically robust. As it can be seen, the TD contrast is always much higher than the CW one,
 170 independently of the depth of the perturbation, and it extends well beyond the CW maximum
 171 depth, allowing to probe tissues down to a depth of 6 cm provided that photons with a delay of
 172 more than 9 ns are detected. As a further proof, the use of the same simulated ideal systems for
 173 tomographic reconstruction (see Figure 1b) of the same absorption perturbation set at a depth of
 174 4 cm completely fails with CW and succeeds with TD, thanks with the much higher contrast at
 175 this depth, while the contrast of the ideal CW system at a depth of 4 cm is considerably below
 176 the detectability threshold of 1%.
 177



178
 179 **Fig. 1** (a) Simulated contrasts for ideal CW- (dashed lines, depth increased by increasing ρ) and TD DO (solid lines,
 180 results at null ρ) systems given by a localized 100% absorption perturbation as a function of its depth inside a
 181 homogenous scattering media ($\mu_a = 0.1 \text{ cm}^{-1}$, $\mu'_s = 10 \text{ cm}^{-1}$). (b) Optical tomography performed using the same ideal
 182 systems and the same perturbation set at a depth of 40 mm (the simulated cubic perturbation is depicted in red).
 183 Reprinted with permission from [40] © The Optical Society.

184
 185 Notwithstanding this impressive scenario, TD systems are presently able to reach a penetration
 186 depth in the order of 2-3 cm. The main conditions to overcome this limit are therefore the
 187 possibility to have wearable systems with: i) dense distribution of probe-hosted (avoiding optical

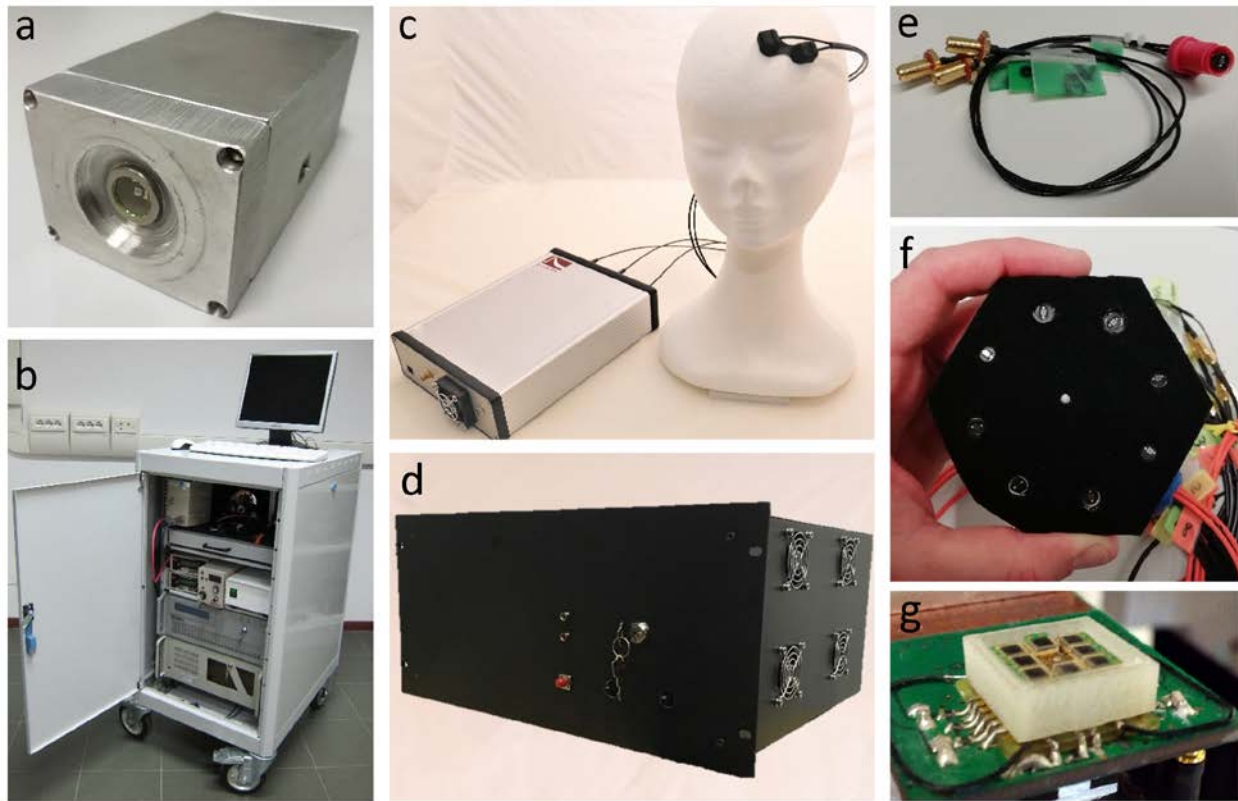
188 fibers) pulsed laser sources to maximize the light power that can be injected into biological
189 media; ii) an equivalent dense distribution of probe-hosted time-resolved single-photon detectors
190 to maximize the amount of collected photons; iii) the time-gating capability to extract the few
191 late photons out of the overwhelming burst of early photons; iv) a high throughput miniaturized
192 timing electronics able to process all photon counts without losses.
193 It is worth noting that, although being highly challenging technological goals, all these have been
194 already demonstrated (or partially demonstrated) in the literature [41]. What is still missing is
195 merging all of them into a single TD system.
196 In a recent work by some of the Authors [40] the possibility to directly place into a wearable
197 probe an array of pulsed vertical-cavity surface emitting lasers has been demonstrated, still using
198 external fast voltage pulse generators to trigger the laser emission. In a later work [42], the use of
199 laser drivers fully integrated into a single silicon chip was introduced in TD DO. Both
200 technologies were validated on phantoms and in-vivo following rigorous protocols for
201 performance assessment of DO systems [43]-[45]. In this way, the assembly of dense
202 arrangements of sources into a small area, if not demonstrated yet, was at least enabled.
203 As a first step towards the second and third conditions, initially another recent work by some of
204 us [40], then other research groups [46],[47] demonstrated the possibility to squeeze the time-
205 gated SPAD technology down to a size compatible with wearable probes. However, SPADs are
206 well known for their limited active area size. Indeed, in Ref. [47] the detector has an active area
207 diameter of 10 μm . In our previous work [40], we made use of a SPAD with a diameter of 200
208 μm . However, in both cases we are still far from the simulated 1 cm^2 collection area.
209 Finally, the last condition is fulfilled in different research prototypes of time-to-digital converters
210 that were published in recent years, allowing to reach throughputs in the order of magnitude of
211 billions of counts per second (cps) in the size of a small piece of silicon [48]-[50].
212

213 **3 The SiPM revolution**

214 It is clear, as discussed before, that the ideal detector for TD DO should exhibit the large active
215 area of PMTs, while showing the typical advantages of SPADs like their compactness and
216 ruggedness. Additionally, good single-photon timing resolution and low noise are required. Even
217 if SiPMs are available since two decades, being optimized for photon-number resolving
218 detection, their use in TD DO was not considered before recent years due to their initial very
219 high dark count rate at the single-photon level, often overcoming 1 Mcps in a 1 mm^2 device, as
220 well as inadequate single-photon timing resolution. However, the SiPM technology underwent
221 strong advancements during the last decade by considerably lowering both DCR and timing
222 jitter. Thus, in 2014 we started exploring these devices for TD DO and this represented a
223 revolution.

224 In a previous work by some of the Authors, the single-photon timing resolution (SPTR) of
225 Hamamatsu Photonics (HP) and Excelitas Technologies (ET) devices has been studied when
226 SiPMs are hosted inside very compact and wearable probes suitable for direct contact with the
227 medium under investigation [51]. In these conditions, from 1.3 x 1.3 mm^2 devices by HP
228 (S13081-050CS) it was possible to achieve a SPTR = 57 ps full-width at half maximum
229 (FWHM), as well as a remarkable SPTR = 67 ps FWHM from 1 x 1 mm^2 devices by ET
230 (C3074011050C). Moving to even larger active areas, from 3 x 3 mm^2 devices by ET
231 (C3074233050C) it was possible to achieve a SPTR = 115 ps FWHM, as well as an SPTR = 135

232 ps FWHM from 3 x 3 mm² devices by HP (S13082-4084). Similarly to SPADs [52], SiPMs
 233 exhibit a first tail in the SPTR response shape with time constant of 60-130 ps (depending on the
 234 considered model) due to photons absorbed within the neutral region of the reverse biased p-n
 235 junction [53] and a second long tail with time constant of 1-4 ns (depending on the considered
 236 model) probably due to the same subtle background phenomena giving rise to the so-called
 237 memory effect in SPADs [54]-[56].
 238 The field of DO relies on well-defined internationally agreed figures of merit for evaluating the
 239 performance of components and system, one of this is the “diffuse optical responsivity” (R),
 240 which can be assessed following the procedure described in [44] using a calibrated phantom. To
 241 give an idea of the improvement in the signal level given by SiPMs, it is worth mentioning that
 242 the R of TD DO systems based on a 1 mm² probe-hosted SiPM can overcome the value of
 243 previous state-of-the-art devices by 1-2 orders of magnitude, and obviously the use of a 9 mm²
 244 can lead to a gain approaching the 3 orders of magnitude.
 245



246 **Fig. 2** SiPM-based TD DO components and systems: (a) single-photon timing module [60], (b) broadband time-
 247 resolved spectroscopy system [61], (c) compact TD fNIRS system [68], (d) 8-wavelength dual detection channel
 248 near-infrared spectroscopy system [70], (e) wearable time-resolved single-photon detector probe [72] and (f)
 249 tomographic probe based on the same detector [73], (g) detection stage of a new optical mammography system [75].
 250

251 SiPMs were in the following validated in different scenarios of possible TD DO applications
 252 like: i) the accurate measurement of optical properties of homogeneous media (highlighting in
 253 particular the capability to linearly follow changes in optical properties and proper uncoupling of
 254 absorption from reduced scattering coefficients), where they showed performance in line with

255 the state of the art [57], ii) the capability of detecting localized perturbations inside the medium
256 in depth, where they showed improved performances thanks to their increased efficiency in the
257 collection of diffused light, thus allowing the detection of a larger number of late-arriving
258 photons [40], iii) the possibility of exploitation in diffuse optical tomography (DOT) systems at a
259 single wavelength to reconstruct 3D maps of optical properties [58], as well as in multispectral
260 DOT to reconstruct 3D maps of different chemical constituents of the sample under investigation
261 [59], in both cases showing impressive performances.

262 Three different parallel branches of SiPM exploitation started: i) replacing PMTs or hybrid
263 PMTs in state-of-the-art bulky systems; ii) designing hybrid systems (still fiber based) between
264 the previous and the next-generation, taking advantage of parallel development of compact laser
265 sources; iii) designing innovative wearable detection chains with high performance thanks to the
266 use of SiPMs directly embedded in the probe in contact with the medium under investigation.

267 To enable the first path, a compact ($5 \times 4 \times 10 \text{ cm}^3$), robust and easy to use SiPM-based single-
268 photon detection module was designed (see Figure 2a) [60]. It embeds an SiPM integrated with a
269 suitable Peltier cooling stage together with the read-out and signal conditioning circuit for
270 avalanche pulses, the biasing electronics and a driver for the thermoelectric cooler. The module
271 uses a detector with a total photosensitive area of 1 mm^2 (with 51% cell fill factor, release 1) or
272 1.7 mm^2 (with 74% cell fill factor, release 2). The detector exhibits an SPTR of $\sim 140 \text{ ps}$ FWHM
273 (release 1) or $\sim 75 \text{ ps}$ FWHM (release 2). This detector was used to replace PMTs in different TD
274 DO systems like a broadband TD optical spectroscopy system (see Figure 2b) [61] and in
275 systems devised for the evaluation of fruit quality [62]. These SiPM-based systems were used in
276 the following years for different pre-clinical studies like the non-invasive characterization of
277 human bones [11] and abdominal fat heterogeneities [63], as well as to retrieve optical properties
278 of basic tissue constituents like collagen [64], elastin [65] and various thyroid chromophores
279 [66]. It is worth mentioning that, in parallel, Hamamatsu Photonics developed a new version of
280 its TD DO system (i.e. the tNIRS-1, a clinical tissue oxygen meter) with 2 SiPM-based detection
281 channels, featuring an overall SPTR of about 1.5 ns FWHM [67].

282 On the second exploitation path, SiPM modules were used to fabricate the first TD system so
283 compact and light-weight to enable unprecedented TD DO application on freely moving
284 subjects, by hosting it into a backpack (see Figure 2c) [68]. Thanks to new compact laser sources
285 (2 wavelengths are embedded for tissue oximetry applications) and to the use of 1 SiPM module
286 and 1 integrated time-to-digital converter (TDC) [69] instead of a classical TCSPC board/system,
287 these devices have roughly the size of a book ($20 \times 16 \times 5 \text{ cm}^3$) and a weight of about 2 kg. Its
288 power consumption lower than 10 W also enables the battery operation. The high performance of
289 lasers, SiPM and TDC, as well as the accurate design of optics and fiber optics components lead
290 to an overall SPTR better than 300 ps at both wavelengths. The same technologies (lasers, SiPM
291 modules and TDCs) were adopted also for developing an 8-wavelength and dual detection
292 channel instrument for diffuse optical spectroscopy (see Figure 2d) [70]. Thanks to further
293 efforts in improving the laser pulse shapes, as well as to the second release of the SiPM module
294 with improved timing resolution, this instrument features an SPTR better than 160 ps FWHM at
295 all the wavelengths, granting high accuracy in the application. Due to a higher system
296 complexity (e.g. the need to embed an optical fiber switch for multiplexing lasers at different
297 wavelengths into the same injection point in the tissue, as well as the need to embed automatic
298 attenuators for each wavelength to adjust the signal to fit the single-photon level) the device has
299 a size of $48 \times 38 \times 20 \text{ cm}^3$, with possibility of being hosted inside a standard 5U 19" rack case.
300 Indeed, this instrument was designed aiming at a primary use inside the LUCA device [71], a

301 multi-modal system exploiting the combination of ultrasound imaging, TD DO and diffuse
302 correlation spectroscopy [16] for characterization of thyroid nodules, aiming at replacing
303 expensive and uncomfortable biopsies with a non-invasive and cheaper examination [29].
304 On the last exploitation path, exploiting the relative simplicity in the front-end electronics
305 required to operate SiPMs, miniaturized single-photon detector modules were designed (see
306 Figure 2e) [72]. These modules require an external bias generator and embed the detector (either
307 a $1 \times 1 \text{ mm}^2$ SiPM C30742-11-050 by ET [72] or a $1.3 \times 1.3 \text{ mm}^2$ SiPM S13081-050CS by HP
308 [73]) together with front-end and avalanche amplification electronics. It is so compact (about 0.6
309 $\times 0.5 \times 2 \text{ cm}^3$) that can be hosted either into small plastic caps compatible with the EEG standard
310 headdress (thus easily allowing fNIRS studies) or into arrangements of different detectors inside
311 a wearable tomographic probe (see Figure 2f). Due to constraints of the compact footprint, these
312 modules feature a SPTR of about 250 ps FWHM. The technology was validated both for muscle
313 oximetry and for monitoring brain functional activations during standard finger-tapping exercises
314 [72] and, in combination with an 8-channel TDC (SC-TDC-1000/08 S, Surface Concept,
315 Germany), for real-time diffuse optical tomography on phantom and in-vivo [73]. Similarly,
316 SiPMs were exploited for improving the performance of a previously developed 7-wavelength
317 optical mammography system. It operates in transmittance geometry, with the breast slightly
318 compressed between two parallel glass plates. In its original conditions, the full breast area was
319 raster-scanned moving simultaneously an injection fiber (where different laser pulses at different
320 wavelengths are multiplexed) and a large area collection fiber bundle, which was bifurcated
321 providing the collected signal to 2 PMTs, one optimized for the visible range and one for the
322 near-infrared range, each one connected to a PC-hosted TCSPC board [74]. SiPMs were used to
323 entirely replace this detection chain [75]. 8 SiPMs with $1.3 \times 1.3 \text{ mm}^2$ active area and 74% fill
324 factor (S13360-1350PE by HP) were arranged in just a $1 \times 1 \text{ cm}^2$ area to act together as a single
325 TD DO detector of equivalent active area of about 10 mm^2 (see Figure 2g), directly replacing the
326 fiber bundle at the collection side. However, to maximize the throughput, each detector is
327 connected to an individual avalanche signal discrimination electronic board and to an
328 independent input channel of a commercially available 8-channel TDC (SC-TDC-1000/08 S,
329 Surface Concept, Germany). In this way, it was possible to reach a gain in signal of minimum 70
330 and maximum 3100 (depending on the wavelength considered) in the spectral range of interest,
331 with a single detector technology replacing both the visible and the near-infrared optimized
332 PMTs.

333 **Conclusions and perspectives**

334 In this paper we have shown how SiPMs recently fostered a revolution in the design of TD DO
335 systems thanks to their superior performance and versatility with respect to PMTs. This
336 revolution is however just at the beginning, being mostly confined where this technology has
337 been first introduced in the field of DO, but it will probably spread all over the world.
338 Additionally, further impressive breakthroughs are expected in the years to come as the full
339 potential of SiPMs still has to be unleashed. Just to mention a couple of examples, while SiPM
340 performance in the visible range is much more attractive than that in the near-infrared one, these
341 detectors have been used to cover the entire spectral range of interest for DO, thus large signal
342 gains are expected when InGaAs SPADs [76],[77] will be used to fabricate structures similar to
343 SiPMs, which seems to be a current trend [78],[79]. Further, we have seen that the conditions for
344 a breakthrough require the combination of a large detection area with fast time-gating capability.

345 Thus, the development of a detector embedding these two features is expected to bring additional
346 advantages and orders of magnitude of gain in the dynamic range of TD DO measurements. This
347 is what is pursued by the H2020 EC-funded SOLUS project [28], which aims at exploiting the
348 combination of ultrasound imaging, shear-wave elastography and diffuse optical tomography for
349 improving the specificity of breast cancer examinations. To this purpose, a compact optode is
350 being developed, which embeds pulsed lasers and a time-gated detector [80]. Some of these
351 optodes will be integrated into a single multimodal probe together with the ultrasound transducer
352 and shear-wave elastography electronics. However, the optode will have a big potential also as a
353 stand-alone object, with envisioned revolutionary impact in TD DO, enabling for the first time a
354 widespread adoption of the technique.

355 **Acknowledgments**

356 The research leading to these results has received partial funding from the EC's H2020
357 Framework Programme under grant agreement No 731877 (SOLUS), No 688303 (LUCA),
358 No 675332 (BITMAP), No 777222 (ATTRACT) and No. 654148 (Laserlab-Europe). SOLUS
359 and LUCA are initiatives of the Photonics Public Private Partnership (www.photonics21.org).

360 **References**

- 361 [1] A. Yodh, B. Chance, Spectroscopy and imaging with diffusing light, *Physics Today*, 48
362 (1995) 34 - 40.
- 363 [2] M. Ferrari, V. Quaresima, Near infrared brain and muscle oximetry: from the discovery
364 to current applications, *Journal of Near Infrared Spectroscopy*, 20 (2012) 1 - 14.
- 365 [3] Y. Yamada, H. Suzuki, Y. Yamashita, Time-domain near-infrared spectroscopy and
366 imaging: a review, *Applied Sciences*, 9 (2019) 1 - 54.
- 367 [4] F. Scholkmann, S. Kleiser, A. J. Metz, R. Zimmermann, J. M. Pavia, U. Wolf, M. Wolf,
368 A review on continuous wave functional near-infrared spectroscopy and imaging
369 instrumentation and methodology, *Neuroimage*, 85 (2014) 6 - 27.
- 370 [5] D. Grosenick, Photon counting in diffuse optical imaging, in: P. Kapusta, M. Wahl, R.
371 Erdmann (Eds.) *Advanced Photon Counting Applications, Methods, Instrumentation*,
372 Springer, 2015, pp. 343 - 365.

- 373 [6] F. Martelli, T. Binzoni, A. Pifferi, L. Spinelli, A. Torricelli, There's plenty of light at
374 the bottom: statistics of photon penetration depth in random media, *Scientific Reports*, 6
375 (2016) 1 - 14.
- 376 [7] R. H. Wilson, K. P. Nadeau, F. B. Jaworski, B. J. Tromberg, A. J. Durkin, Review of
377 short-wave infrared spectroscopy and imaging methods for biological tissue
378 characterization, *Journal of Biomedical Optics*, 20 (2015) 1 - 10.
- 379 [8] A. Torricelli, D. Contini, A Pifferi, M. Caffini, R. Re, L. Zucchelli, L. Spinelli, Time
380 domain functional NIRS imaging for human brain mapping, *Neuroimage* 85 (2014) 28 -
381 50.
- 382 [9] D. Grosenick, H. Rinneberg, R. Cubeddu, P. Taroni, Review of optical breast imaging
383 and spectroscopy, *Journal of Biomedical Optics*, 21 (2016) 1 - 27.
- 384 [10] C. Lindner, M. Mora, P. Farzam, M. Squarcia, J. Johansson, U. M. Weigel, I. Halperin,
385 F. A. Hanzu, and T. Durduran, Diffuse optical characterization of the healthy human
386 thyroid tissue and two pathological case studies, *PLoS One*, 11 (2016) 1 -22.
- 387 [11] S. Konugolu Venkata Sekar, M. Pagliazzi, E. Negro, F. Martelli, A. Farina, A. Dalla
388 Mora, C. Lindner, P. Farzam, N. Pérez-Álvarez, J. Puig, P. Taroni, A. Pifferi, T.
389 Durduran, In vivo, non-invasive characterization of human bone by hybrid broadband
390 (600-1200 nm) diffuse optical and correlation spectroscopies, *PLoS One*, 11 (2016) 1-
391 16.
- 392 [12] A. Torricelli, L. Spinelli, D. Contini, M. Vanoli, A. Rizzolo, P. Eccher Zerbini, Time-
393 resolved reflectance spectroscopy for non-destructive assessment of food quality,
394 *Sensing and Instrumentation for Food Quality and Safety* 2 (2008) 82 - 89.

- 395 [13] I. Bargigia, A. Nevin, A. Farina, A. Pifferi, C. D'Andrea, M. Karlsson, P. Lundin, G.
396 Somesfalean, S. Svanberg, Diffuse optical techniques applied to wood characterization,
397 Journal of Near Infrared Spectroscopy, 21 (2013) 259 - 268.
- 398 [14] D. Khoptyar, A. A. Subash, S. Johansson, M. Saleem, A. Sparén, J. Johansson, S.
399 Andersson-Engels, Broadband photon time-of-flight spectroscopy of pharmaceuticals
400 and highly scattering plastics in the VIS and close NIR spectral ranges, Optics Express,
401 21 (2013) 20941 - 20953.
- 402 [15] C. D'Andrea, E. A. Obraztsova, A. Farina, P. Taroni, G. Lanzani, A. Pifferi, Absorption
403 spectroscopy of powdered materials using time-resolved diffuse optical methods,
404 Applied Optics, 51 (2012) 7858 - 7863.
- 405 [16] T. Durduran, R. Choe, W. B. Baker, A. G. Yodh, Diffuse optics for tissue monitoring
406 and tomography, Reports on Progress in Physics, 73 (2010) 1 - 44.
- 407 [17] W. Becker, Advanced Time-Correlated Single Photon Counting Techniques, Springer-
408 Verlag, New York, 2005.
- 409 [18] S. Del Bianco, F. Martelli, G. Zaccanti, Penetration depth of light re-emitted by a
410 diffusive medium: Theoretical and experimental investigation, Physics in Medicine and
411 Biology, 47 (2002) 4131 - 4144.
- 412 [19] J. Steinbrink, H. Wabnitz, H. Obrig, A. Villringer, H. Rinneberg, Determining changes
413 in NIR absorption using a layered model of the human head, Physics in Medicine and
414 Biology, 46 (2001) 879 - 896.
- 415 [20] J. Selb, J. J. Stott, M. A. Franceschini, A. G. Sorensen, D. A. Boas, Improved sensitivity
416 to cerebral hemodynamics during brain activation with a time-gated optical system:

417 analytical model and experimental validation, *Journal of Biomedical Optics*, 10 (2005)
418 1 - 12.

419 [21] D. Contini, L. Spinelli, A. Torricelli, A. Pifferi, R. Cubeddu, Novel method for depth-
420 resolved brain functional imaging by time-domain NIRS, *Proceedings of SPIE*, 6629
421 (2007) 1 - 7.

422 [22] A. Torricelli, A. Pifferi, L. Spinelli, R. Cubeddu, F. Martelli, S. Del Bianco, G.
423 Zaccanti, Time-resolved reflectance at null source-detector separation: improving
424 contrast and resolution in diffuse optical imaging, *Physics Review Letters*, 95 (2005) 1 -
425 4.

426 [23] A. Pifferi, A. Torricelli, L. Spinelli, D. Contini, R. Cubeddu, F. Martelli, G. Zaccanti, A.
427 Tosi, A. Dalla Mora, F. Zappa, S. Cova, Time-resolved diffuse reflectance using small
428 source-detector separation and fast single-photon gating, *Physics Review Letters* 100
429 (2008) 1 - 4.

430 [24] M. Mazurenka, L. Di Sieno, G. Boso, D. Contini, A. Pifferi, A. Dalla Mora, A. Tosi, H.
431 Wabnitz, R. Macdonald, Non-contact in vivo diffuse optical imaging using a time-gated
432 scanning system, *Biomedical Optics Express* 4 (2013) 2257 - 2268.

433 [25] E. Alerstam, T. Svensson, S. Andersson-Engels, L. Spinelli, D. Contini, A. Dalla Mora,
434 A. Tosi, F. Zappa, A. Pifferi, Single-fiber diffuse optical time-of-flight spectroscopy,
435 *Optics Letters*, 37 (2012) 2877 – 2879.

436 [26] A. Dalla Mora, A. Tosi, F. Zappa, S. Cova, D. Contini, A. Pifferi, L. Spinelli, A.
437 Torricelli, R. Cubeddu, Fast-gated single-photon avalanche diode for wide dynamic
438 range near infrared spectroscopy, *IEEE Journal of Selected Topics in Quantum*
439 *Electronics*, 16 (2010)1023 - 1030.

- 440 [27] M. Buttafava, G. Boso, A. Ruggeri, A. Dalla Mora, A. Tosi, Time-gated single-photon
441 detection module with 110 ps transition time and up to 80 MHz repetition rate, Review
442 of Scientific Instruments, 85 (2014) 1 - 8.
- 443 [28] www.solus-project.eu (accessed on 25/10/2019)
- 444 [29] www.luca-project.eu (accessed on 25/10/2019)
- 445 [30] www.bitmap-itn.eu (accessed on 25/10/2019)
- 446 [31] attract-eu.com (accessed on 25/10/2019)
- 447 [32] www.laserlab-europe.eu (accessed on 25/10/2019)
- 448 [33] E. Ohmae, M. Oda, T. Suzuki, Y. Yamashita, Y. Kakihana, A. Matsunaga, Y. Kanmura,
449 M. Tamura, Clinical evaluation of time-resolved spectroscopy by measuring cerebral
450 hemodynamics during cardiopulmonary bypass surgery, Journal of Biomedical Optics
451 12 (2007) 1 - 9.
- 452 [34] A. T. Eggebrecht, S. L. Ferradal, A. Robichaux-Viehoever, M. S. Hassanpour, H.
453 Deghani, A. Z. Snyder, T. Hershey, J. P. Culver, Mapping distributed brain function
454 and networks with diffuse optical tomography, Nature Photonics, 8 (2014) 448 - 454.
- 455 [35] S. Andersson-Engels, R. Berg, A. Persson, S. Svanberg, Multispectral tissue
456 characterization with time-resolved detection of diffusely scattered white light, Optics
457 Letters, 18 (1993) 1697 - 1699.
- 458 [36] M. Kacprzak, A. Liebert, P. Sawosz P, N. Żolek, R. Maniewski, Time-resolved optical
459 imager for assessment of cerebral oxygenation, Journal of Biomedical Optics 12 (2007)
460 1 - 14.

- 461 [37] H. Wabnitz, M. Moeller, A. Liebert, H. Obrig, J. Steinbrink, R. Macdonald, Time-
462 resolved near-infrared spectroscopy and imaging of the adult human brain, *Advances in*
463 *Experimental Medicine and Biology*, 662 (2009) 143 - 148.
- 464 [38] J. C. Hebden, M. Varela, S. Magazov, N. Everdell, A. Gibson, J. Meek, T. Austin,
465 Diffuse optical imaging of the newborn infant brain, *Proceedings of 9th IEEE*
466 *International Symposium on Biomedical Imaging*, 1 (2012) 503 - 505.
- 467 [39] A. Puszka, L. Di Sieno, A. Dalla Mora, A. Pifferi, D. Contini, A. Planat-Chrétien, A.
468 Koenig, G. Boso, A. Tosi, L. Hervé, J.-M. Dinten, Spatial resolution in depth for time-
469 resolved diffuse optical tomography using short source-detector separations, *Biomedical*
470 *Optics Express* 6 (2015) 1 - 10.
- 471 [40] A. Dalla Mora, D. Contini, S. Arridge, F. Martelli, A. Tosi, G. Boso, A. Farina, T.
472 Durduran, E. Martinenghi, A. Torricelli, A. Pifferi, Towards next-generation time-
473 domain diffuse optics for extreme depth penetration and sensitivity, *Biomedical Optics*
474 *Express*, 6 (2015) 1749 - 1760.
- 475 [41] A. Pifferi, D. Contini, A. Dalla Mora, A. Farina, L. Spinelli, A. Torricelli, New frontiers
476 in time-domain diffuse optics, a review, *Journal of Biomedical Optics*, 21 (2016) 1 - 17.
- 477 [42] L. Di Sieno, J. Nissinen, L. Hallman, E. Martinenghi, D. Contini, A. Pifferi, J.
478 Kostamovaara, A. Dalla Mora, Miniaturized pulsed laser source for time-domain diffuse
479 optics routes to wearable devices, *Journal of Biomedical Optics*, 22 (2017) 1 - 9.
- 480 [43] A. Pifferi, A. Torricelli, A. Bassi, P. Taroni, R. Cubeddu, H. Wabnitz, D. Grosenick, M.
481 Möller, R. Macdonald, J. Swartling, T. Svensson, S. Andersson-Engels, R. L. P. van
482 Veen, H. J. C. M. Sterenborg, J.-M. Tualle, H. L. Nghiem, S. Avriillier, M. Whelan, and

483 H. Stamm, Performance assessment of photon migration instruments: the MEDPHOT
484 protocol, *Applied Optics*, 44 (2005) 2104–2114.

485 [44] H. Wabnitz, D. R. Taubert, M. Mazurenka, O. Steinkellner, A. Jelzow, R. Macdonald,
486 D. Milej, P. Sawosz, M. Kacprzak, A. Liebert, R. Cooper, J. Hebden, A. Pifferi, A.
487 Farina, I. Bargigia, D. Contini, M. Caffini, L. Zucchelli, L. Spinelli, R. Cubeddu, A.
488 Torricelli, Performance assessment of time-domain optical brain imagers, part 1: basic
489 instrumental performance protocol, *Journal of Biomedical Optics* 19 (2014) 1 - 12.

490 [45] H. Wabnitz, A. Jelzow, M. Mazurenka, O. Steinkellner, R. Macdonald, D. Milej, N.
491 Żolek, M. Kacprzak, P. Sawosz, R. Maniewski, A. Liebert, S. Magazov, J. Hebden, F.
492 Martelli, P. Di Ninni, G. Zaccanti, A. Torricelli, D. Contini, R. Re, L. Zucchelli, L.
493 Spinelli, R. Cubeddu, and A. Pifferi, Performance assessment of time-domain optical
494 brain imagers, part 2: nEUROPt protocol, *Journal of Biomedical Optics* 19 (2014) 1 -
495 12.

496 [46] S. Saha, Y. Lu, S. Weyers, M. Sawan, F. Lesage, Compact fast optode-based probe for
497 single-photon counting applications, *IEEE Photonics Technology Letters*, 30 (2018)
498 1515 - 1518.

499 [47] S. Saha, S. Burri, C. Bruschini, E. Charbon, F. Lesage, M. Sawan, Time domain NIRS
500 optode based on null/small source-detector distance for wearable applications,
501 *Proceedings of 2019 IEEE Custom Integrated Circuits Conference*, 1 (2019) 1-8.

502 [48] D. Tyndall, B. R. Rae, D. Day-Uei Li, J. Arlt, A. Johnston, J. A. Richardson, R. K.
503 Henderson, A high-throughput time-resolved mini-silicon photomultiplier with
504 embedded fluorescence lifetime estimation in 0.13 μm CMOS, *IEEE IEEE Transactions*
505 *on Biomedical Circuits and Systems*, 6 (2012) 562 - 570.

- 506 [49] N. A. W. Dutton, S. Gneccchi, L. Parmesan, A. J. Holmes, B. Rae Lindsay, A. Grant, R.
507 K. Henderson, 11.5 A time-correlated single-photon-counting sensor with 14GS/S
508 histogramming time-to-digital converter, 2015 IEEE International Solid-State Circuits
509 Conference - (ISSCC) Digest of Technical Papers, 1 (2015) 1 - 3.
- 510 [50] N. Krstajić, S. Poland, J. Levitt, R. Walker, A. Erdogan, S. Ameer-Beg, R. K.
511 Henderson, 0.5 billion events per second time correlated single photon counting using
512 CMOS SPAD arrays, Optics Letters, 40 (2015) 4305 - 4308.
- 513 [51] E. Martinenghi, A. Dalla Mora, D. Contini, A. Farina, F. Villa, A. Torricelli, A. Pifferi,
514 Spectrally resolved single-photon timing of silicon photomultipliers for time-domain
515 diffuse optics, IEEE Photonics Journal, 7 (2015) 1 - 12.
- 516 [52] A. Gulinatti, P. Maccagnani, I. Rech, M. Ghioni, S. Cova, 35 ps time resolution at room
517 temperature with large area single photon avalanche diodes, Electronics Letters, 41
518 (2005) 272 - 274.
- 519 [53] D. Contini, A. Dalla Mora, L. Spinelli, A. Farina, A. Torricelli, R. Cubeddu, F. Martelli,
520 G. Zaccanti, A. Tosi, G. Boso, F. Zappa, A. Pifferi, Effects of time-gated detection in
521 diffuse optical imaging at short source-detector separation, Journal of Physics D:
522 Applied Physics, 48 (2015) 1 - 11.
- 523 [54] A. Dalla Mora, D. Contini, A. Pifferi, R. Cubeddu, A. Tosi, F. Zappa, Afterpulse-like
524 noise limits dynamic range in time-gated applications of thin-junction silicon single-
525 photon avalanche diode, Applied Physics Letters, 100 (2012) 1 - 4.
- 526 [55] A. Dalla Mora, A. Tosi, D. Contini, L. Di Sieno, G. Boso, F. Villa, A. Pifferi, Memory
527 effect in silicon time-gated single-photon avalanche diodes, Journal of Applied Physics,
528 117 (2015) 1 - 7.

- 529 [56] A. Behera, L. Di Sieno, A. Pifferi, F. Martelli, A. Dalla Mora, Instrumental, optical and
530 geometrical parameters affecting time-gated diffuse optical measurements: a systematic
531 study, *Biomedical Optics Express*, 9 (2018) 5524 - 5542.
- 532 [57] A. Dalla Mora, E. Martinenghi, D. Contini, A. Tosi, G. Boso, T. Durduran, S. Arridge,
533 F. Martelli, A. Farina, A. Torricelli, A. Pifferi, Fast silicon photomultiplier improves
534 signal harvesting and reduces complexity in time-domain diffuse optics, *Optics Express*,
535 23 (2015) 13937 - 13946.
- 536 [58] L. Di Sieno, J. Zouaoui, L. Hervé, A. Pifferi, A. Farina, E. Martinenghi, J. Derouard, J.-
537 M. Dinten, A. Dalla Mora, Time-domain diffuse optical tomography using silicon
538 photomultipliers: feasibility study, *Journal of Biomedical Optics*, 21 (2016) 1 - 10.
- 539 [59] J. Zouaoui, L. Di Sieno, L. Hervé, A. Pifferi, A. Farina, A. Dalla Mora, J. Derouard, J.-
540 M. Dinten, Chromophore decomposition in multispectral time-resolved diffuse optical
541 tomography, *Biomedical Optics Express*, 8 (2017) 4772 - 4787.
- 542 [60] E. Martinenghi, L. Di Sieno, D. Contini, M. Sanzaro, A. Pifferi, A. Dalla Mora, Time-
543 resolved single-photon detection module based on silicon photomultiplier: a novel
544 building block for time-correlated measurement systems, *Review of Scientific*
545 *Instruments*, 87 (2016) 1 - 8.
- 546 [61] S. Konugolu Venkata Sekar, A. Dalla Mora, I. Bargigia, E. Martinenghi, C. Lindner, P.
547 Farzam, M. Pagliuzzi, T. Durduran, P. Taroni, A. Pifferi, A. Farina, Broadband (600-
548 1350 nm) time resolved diffuse optical spectrometer for clinical use, *IEEE Journal of*
549 *Selected Topics in Quantum Electronics*, 22 (2016) 1 - 9.
- 550 [62] A. Torricelli, D. Contini, A. Dalla Mora, E. Martinenghi, D. Tamborini, F. Villa, A.
551 Tosi, L. Spinelli, Recent advances in time-resolved NIR spectroscopy for

552 nondestructive assessment of fruit quality, *Chemical Engineering Transactions*, 44
553 (2015) 43 - 48.

554 [63] P. Lanka, A. Farina, S. Konugolu Venkata Sekar, C. Guadagno, L. Spinelli, P. Taroni,
555 R. Cubeddu, E. Nisoli, A. Pifferi, Multidistance time domain diffuse optical
556 spectroscopy in the assessment of abdominal fat heterogeneity, *Proceedings of SPIE*,
557 10685 (2018) 1 - 7.

558 [64] S. Konugolu Venkata Sekar, I. Bargigia, A. Dalla Mora, P. Taroni, A. Ruggeri, A. Tosi,
559 A. Pifferi, A. Farina, Diffuse optical characterization of collagen absorption from 500 to
560 1700 nm, *Journal of Biomedical Optics*, 22 (2017) 1 - 6.

561 [65] S. Konugolu Venkata Sekar, J. Sin Beh, A. Farina, A. Dalla Mora, A. Pifferi, P. Taroni
562 Broadband diffuse optical characterization of elastin for biomedical applications,
563 *Biophysical Chemistry*, 229 (2017) 130 - 134.

564 [66] S. Konugolu Venkata Sekar, A. Farina, A. Dalla Mora, C. Lindner, M. Pagliuzzi, M.
565 Mora, G. Aranda, H. Dehghani, T. Durduran, P. Taroni, A. Pifferi, Broadband (550-1350
566 nm) diffuse optical characterization of thyroid chromophores, *Scientific Reports*, 8
567 (2018) 1 - 8.

568 [67] S. Fujisaka, T. Ozaki, T. Suzuki, T. Kamada, K. Kitazawa, M. Nishizawa, A.
569 Takahashi, S. Suzuki, A clinical tissue oximeter using NIR time-resolved spectroscopy,
570 *Advances in Experimental Medicine and Biology*, 876 (2016) 427 - 433.

571 [68] M. Buttafava, E. Martinenghi, D. Tamborini, D. Contini, A. Dalla Mora, M. Renna, A.
572 Torricelli, A. Pifferi, F. Zappa, A. Tosi, A compact two-wavelength time-domain NIRS
573 system based on SiPM and pulsed diode lasers, *IEEE Photonics Journal*, 9 (2017) 1 - 14.

- 574 [69] B. Markovic, S. Tisa, F. A. Villa, A. Tosi, and F. Zappa, A high-linearity, 17 ps
575 precision time-to-digital converter based on a single-stage Vernier delay loop fine
576 interpolation, IEEE Transactions on Circuits and Systems I: Regular Papers 60 (2013)
577 557 - 569.
- 578 [70] M. Renna, M. Buttafava, A. Behera, M. Zanoletti, L. Di Sieno, A. Dalla Mora, D.
579 Contini, A. Tosi, Eight-wavelength, dual detection-channel instrument for near-infrared
580 time-resolved diffuse optical spectroscopy, IEEE Journal of Selected Topics in
581 Quantum Electronics, 25 (2019) 1 - 11.
- 582 [71] L. Cortese, G. Aranda, M. Buttafava, D. Contini, A. Dalla Mora, S. de Fraguier, H.
583 Dehghani, E. Garcia, R. Gomis, F. Hanzu, K. Krischak, G. Lo Presti, M. Mora, A.
584 Pifferi, M. Renna, B. Rosinski, S. Konugolu Venkata Sekar, M. Squarcia, P. Taroni, A.
585 Tosi, U.M. Weigel, S. Wojtkiewicz, M. Zanoletti, P. Zolda, T. Durduran, The LUCA
586 device - laser and ultrasound co-analyzer for thyroid nodules, Proceedings of SPIE,
587 11074 (2019) 1 - 3.
- 588 [72] R. Re, E. Martinenghi, A. Dalla Mora, D. Contini, A. Pifferi, A. Torricelli, Probe-hosted
589 silicon photomultipliers for time-domain functional near-infrared spectroscopy:
590 phantom and in vivo tests, Neurophotonics, 3 (2016) 1 - 9.
- 591 [73] A. Farina, S. Tagliabue, L. Di Sieno, E. Martinenghi, T. Durduran, S. Arridge, F.
592 Martelli, A. Torricelli, A. Pifferi, A. Dalla Mora, Time-domain functional diffuse
593 optical tomography system based on fiber-free silicon photomultipliers, Applied
594 Sciences, 7 (2017) 1 - 18.

- 595 [74] P. Taroni, A. Pifferi, E. Salvagnini, L. Spinelli, A. Torricelli, R. Cubeddu, Seven-
596 wavelength time-resolved optical mammography extending beyond 1000 nm for breast
597 collagen quantification, *Optics Express*, 17 (2009) 15932 - 15946.
- 598 [75] E. Ferocino, E. Martinenghi, A. Dalla Mora, A. Pifferi, R. Cubeddu, P. Taroni, High
599 throughput detection chain for time domain optical mammography, *Biomedical Optics*
600 *Express*, 9 (2018) 755 - 770.
- 601 [76] M. A. Itzler, R. Ben-Michael, C.-F. Hsu, K. Slomkowski, A. Tosi, S. Cova, F. Zappa, R.
602 Ispasoiu, Single photon avalanche diodes (SPADs) for 1.5 μm photon counting
603 applications, *Journal of Modern Optics*, 54 (2007) 283 - 304.
- 604 [77] A. Tosi, F. Acerbi, A. Dalla Mora, M. A. Itzler, X. Jiang, Active area uniformity of
605 InGaAs/InP single-photon avalanche diodes, *IEEE Photonics Journal*, 3 (2011) 31 - 41.
- 606 [78] X. Jiang, M. A. Itzler, B. Nyman, K. Slomkowski, Negative feedback avalanche diodes
607 for near-infrared single-photon detection, *Proceedings of SPIE*, 7320 (2009) 1 - 10.
- 608 [79] J. Zhang, M. A. Itzler, H. Zbinden, J.-W. Pan, Advances in InGaAs/InP single-photon
609 detector systems for quantum communication, *Light: Science & Applications*, 4 (2015)
610 1 - 13.
- 611 [80] P. Taroni, P. Gordebeke, A. Dalla Mora, A. Tosi, A. Pifferi, J.-M. Dinten, M. Perriollat,
612 D. Savery, H. Sportouche, B. Rosinski, S. Arridge, A. Giudice, S. Tisa, E. Venturini, P.
613 Panizza, P. Zolda, A. Flocke, A multimodal system for the diagnosis of breast cancer:
614 the SOLUS project, *Diagnostic Imaging Europe*, 34 (2018) 20 - 22.